# We are IntechOpen,
# the world's leading publisher of
# Open Access books
# Built by scientists, for scientists

## 4,800
Open access books available

## 122,000
International authors and editors

## 135M
Downloads

Our authors are among the

## 154
Countries delivered to

## TOP 1%
most cited scientists

## 12.2%
Contributors from top 500 universities

CLARIVATE ANALYTICS
**BOOK CITATION INDEX**
INDEXED

**WEB OF SCIENCE**™

Selection of our books indexed in the Book Citation Index
in Web of Science™ Core Collection (BKCI)

# Interested in publishing with us?
# Contact book.department@intechopen.com

# Climate Change Assessment Due to Long Term Soil Moisture Change and Its Applicability Using Satellite Observations

Hui Lu, Toshio Koike, Tetsu Ohta,
Katsunori Tamagawa, Hideyuki Fujii and David Kuria

Additional information is available at the end of the chapter

## 1. Introduction

In researches related to the climate change, soil moisture is serving as an excellent environmental indicator controlling and regulating the interaction between the atmosphere and the land surface (Betts et al. 1996; Entekhabi et al. 1996). Soil moisture controls the ratio of runoff and infiltration (Delworth & Manabe 1988; Wagner et al. 2003), decides the energy fluxes (Entekhabi et al. 1996; Prigent et al. 2005) and influents vegetation development and then carbon cycle (Pastor & Post 1986; Melillo et al. 2002). Moreover, soil moisture is also an important factor in animal and plant productivity and it can even constrain to the interaction between natural system and anthropic activity. Therefore, the distribution pattern of soil moisture, both spatial and temporal, is the key of climate system modelling. Moreover, a long term soil moisture data set on a region scale therefore could provide valuable information for researches such as climate change and global warming (Seneviratne et al. 2006), and then improve the weather forecasting (Beljaars et al. 1996; Schar et al. 1999) and water resources management.

Traditionally, soil moisture is measured at point scale through filed samplings and/or automatic instruments, for example, Time Domain Reflector (TDR). These methods are commonly used to provide accurate and continuous soil moisture information and adopted by the meteorology, hydrology and agriculture stations. Through such point scale measurement, long term and accurate soil moisture information was collected. Such information is useful in climate change study, but it is only at point scale and is only available at limited locations.

Contrary to the limitations of *in situ* measurements, numerical models can provide continuous estimates of soil moisture over the entire soil profile at any scale. Therefore, the numerical simulation, in which meteorological observations and land surface models are employed, became the main approach for studying soil moisture variation. However, the limitations of the numerical simulation approach such as the simplification of physical processes, the uncertainty in parameters and the biases in atmospheric data are significant. Consequently, the accuracy of simulation results is highly dependent on the quality of the atmospheric data from which the uncertainties and biases were inherited.

Unlike model simulations, remote sensing is able to provide land surface soil moisture observations that do not rely on atmospheric variables. This independence is very important to ensure objectivity of the climate change impact assessment. Satellite remote sensing offers a possibility to measure surface soil moisture at regional, continental and even global scales. Although surface soil moisture can be estimated indirectly from visible/IR remote sensing data (Verstraeten et al. 2006; Gillies & Carlson 1995), it failed to produce routinely soil moisture map mainly due to factors inherent in optical remote sensing, such as atmosphere effects, cloud masking effects and vegetation cover masking effects. Currently, the most popular technique is the microwave remote sensing which provides a means of direct surface soil moisture measurement for a range of vegetation cover conditions (Oh, Sarabandi & Ulaby 1992; Kerr et al. 2001; Paloscia et al. 2008; Njoku & Chan 2006). The scientific basis of microwave soil moisture remote sensing is the strong relationship between the soil dielectric properties and its liquid moisture content (Hipp 1974; Wang & Schmugge 1980). Moreover, extra advantages of microwave remote sensing include: (1) long wavelength in microwave region which enable the low frequency microwave signals to penetrate clouds and to provide physical information of the land surface; and (2) independent of illumination source which enables the spaceborne sensors to observe earth all-day with all-weather coverage.

There are two approaches through which microwave remote sensing estimates surface soil moisture: active ways by Radar and/or SAR with high spatial resolution (in the order of ten to hundred meters) and long revisiting period (about 1 month), passive ways by radiometers with coarse resolution (~ order of 10 km) and frequent temporal coverage (daily or bi-daily). Considering the temporal resolution requirement of the meteorological and hydrological modelling, passive ways are more suitable for the application in these fields. Passive microwave remote sensing has been recognized as a potential method for measuring soil moisture with a large spatial coverage, while the sensors operated at low frequencies have been acknowledged to be capable to estimate soil moisture reliably (Njoku & Li 1999; Wigneron et al. 1998; Njoku & Entekhabi 1996). For instance, the Advanced Microwave Scanning Radiometer for the Earth Observing System (AMSR-E) is believed to offer state-of-the-art soil moisture estimation through the combination of low frequency observations at 6.9, 10.65 and 18.7 GHz (Paloscia, Macelloni & Santi 2006; Njoku et al. 2003). In terms of soil moisture temporal distribution, the Special Sensor Microwave/Imager (SSM/I) equipped on Defense Meteorological Satellite Program (DMSP) satellites, measuring the brightness temperature of the earth at 19.35, 22.235, 37 and 85.5 GHz with a history around 20 years, is

highly expected to provide long-term global soil moisture estimation (Paloscia et al. 2001; Prigent et al. 2000; Jackson 1997; Hollinger et al. 1987). Before SSM/I, the Scanning Multichannel Microwave radiometer (SMMR) on board Nimbus-7 Pathfinder (Gloersen & Barath 1977), provides brightness temperature observation at 6.6, 10.7, 18.0, 21 and 37 GHz from 1978-1987.

In this study, we investigated the applicability of the remotely sensed soil moisture in climate change studies. We retrieved long term soil moisture over the whole Africa continent from SSM/I by using a revised algorithm. The long term soil moisture data set was analyzed to demonstrate the advantages of passive microwave remote sensing in supporting the climate change studies. The results were compared with the reanalysis data subset from ECMWF (European Centre for Medium-Range Weather Forecasts) 40-year Reanalysis data (ERA-40) and The National Centers for Environmental Prediction/National Center for Atmospheric Research (NCEP/NCAR) reanalysis data.

The paper is organized as follows. In Section 2 we describe the structure of the soil moisture retrieving algorithm. Section 3 presents a short introduction to the study region and used data.Section 4 discusses the application case by using SSM/I soil moisture data over Africa. Section 5 ends this paper with some concluding remarks.

## 2. Soil moisture retrieval algorithm

The soil moisture retrieval algorithm for passive microwave remote sensing data consists of three parts: a forward model, a retrieving algorithm and the ancillary data set.

### 2.1. The forward model: radiative transfer model

Our algorithm is based on a look up table, which is a database of brightness temperature simulated by a radiative transfer model for various possible conditions. The quality of retrieved soil moisture, therefore, is heavily dependent on the performance of the radiative transfer model. So, the main task of our algorithm development is to develop a physically-based soil moisture retrieval algorithm, which is able to estimate soil moisture content from low frequency passive microwave remote sensing data and to overcome the misrepresent problems occurred in dry areas.

#### 2.1.1. The radiative transfer process for land surface remote sensing

For the land surface remote sensing by spaceborne microwave radiometers, the radiative transfer process from land to space can be divided into as four stages as follows:

1.  Radiative transfer inside soil media

The initial incident energy is treated as the one starting from the deep soil layer, which propagates through many soil layers, attenuating by the soil absorption effects (dominative at wet cases) and volume scattering effects (dominative at dry cases), experiencing multi-reflection effects between the interfaces of soil layers, finally reaching the soil/air interface.

2.    Surface scattering process at soil/air interface

At the soil/air interface, the surface scattering influences this upward initial radiation by changing its direction, magnitude and polarization status. At the same time, the downward radiation from the cosmic background, atmosphere, precipitation and canopy are reflected by the air/soil interface, and parts of the reflected radiation propagate along the same direction as that emitted from the soil layers.

The upward radiation just above the soil/air interface, therefore, is not only the product of soil medium but also the product of downward radiation.

3.    Radiative transfer inside vegetation layers

After leaving the soil/air interface, the upward radiation propagates through the canopy layer (if there are vegetations), experiences the volume scattering effects from the leaves and stems of vegetations and the multi-reflection effects between canopy/air and soil/air interfaces. At the same time, parts of the upward radiation from vegetations join our target radiation.

4.    Radiative transfer inside atmosphere layers

After transmitting from vegetation layer, the radiation continues its way, traversing the cloud and precipitation layers, affected by the absorptive atmosphere gases, scattered by precipitation drops, incorporating the emission from surroundings, finally detected by the sensors boarded on satellites.

The story of radiative transfer is so complicate that make it necessary to simplify the process to make it computable. In microwave region, the reflectivity of the air/soil interface is generally small. The downward radiation from vegetation and rainfall, which is reflected by the soil surface, therefore, is neglected. Moreover, for the lower frequencies region of microwave, the atmosphere is transparent. Finally, after neglecting all the downward radiation and parts of upward radiation from surroundings, the radiative transfer model is written as:

$$T_b = T_{bs}e^{-\tau_c}e^{-\tau_r} + (1-\omega_c)(1-e^{-\tau_c})T_c e^{-\tau_r} + \int (1-\omega_r(R))(1-e^{-\tau_r(R)})T_r(R)dR \qquad (1)$$

where $T_{bs}$ is the emission of the soil layer, $T_c$ is the vegetation temperature, $T_r$ is the temperature of precipitation droplets, $\tau_c$ and $\omega_c$ are the vegetation opacity and single scattering albedo, and $\tau_r$ and $\omega_r$ are the opacity and single scattering albedo of precipitation.

For the frequencies less than 18GHz, equation (1) can be even simplified by omitting the precipitation layer, as:

$$T_b = T_{bs}e^{-\tau_c} + (1-\omega_c)(1-e^{-\tau_c})T_c \qquad (2)$$

### 2.1.2. Radiative process inside soil media: profile effects and volume scatting effects

Microwave can penetrate into soil media, especially for dry cases, in which the penetration depth of C-band is about several centimeters. The soil moisture observed by microwave

remote sensing, therefore, is inside a soil media with a volume of several centimeters depth. The radiative transfer process inside a soil media includes various effects, such as moisture and temperature profile effects and the volume scattering effects of dry soil particles. To simulate these effects, the dielectric constant model should be addressed at first.

1.   Dielectric constant model of soil

In the view of microwave, soil is a multi-phase mixture, with a dielectric constant decided by moisture content, bulk density, soil textural composition, soil temperature and salinity. In our algorithm, the dielectric constant of soil is calculated using Dobson model (Dobson et al. 1985):

$$\varepsilon_{soil}^{\alpha} = 1 + \frac{\rho_b}{\rho_{ss}}(\varepsilon_{ss}^{\alpha} - 1) + m_v^{\beta}\varepsilon_{fw}^{\alpha} - m_v \tag{3}$$

where $\rho_b$ is the bulk density of sand, $\rho_{ss}$ = 2.71 is the density of solid sand particle; $\varepsilon_{ss}$ = (4.7, 0.0) is the dielectric constant of sand particle; $m_v$ is the volumetric water content; $\varepsilon_{fw}$ is the dielectric constant of free water, can be calculated by the model proposed by Ray (1972); $\alpha$=0.65 is an empirical parameter; and $\beta$ is a soil texture dependent parameter as follows:

$$\beta = 1.09 - 0.11S + 0.18C \tag{4}$$

where $S$ and $C$ are the sand and clay fraction of the soil, respectively.

2.   Profile effects of soil media

The heterogeneity inside soil media causes the so-called profile effects. The profile effects can be accounted for by using the simple zero-order noncoherent model proposed by Schmugge and Choudhury (1981) or by more complicate first-order noncoherent model given by Burke et al. (1979). The volume scattering effects inside soil media are not included in both models.

In order to include the volume scattering effects, a more complicate model was adopted in our algorithm. We assumed that the soil has a multi-layer structure and is composed of many plane-parallel and azimuthally symmetric soil slabs with spherical scattering particles. The radiative transfer process in a plane-parallel and azimuthally symmetric soil slab with spherical scattering particles can be expressed as (Tsang & Kong 1977):

$$\mu\frac{d}{d\tau}\begin{bmatrix} I_v(\tau,\mu) \\ I_h(\tau,\mu) \end{bmatrix} = \begin{bmatrix} I_v(\tau,\mu) \\ I_h(\tau,\mu) \end{bmatrix} - (1-\omega_0)B(\tau)\begin{bmatrix} 1 \\ 1 \end{bmatrix} - \frac{\omega_0}{2}\int_{-1}^{1}\begin{bmatrix} P_{VV} & P_{VH} \\ P_{HV} & P_{HH} \end{bmatrix}\begin{bmatrix} I_v(\tau,\mu') \\ I_h(\tau,\mu') \end{bmatrix}d\mu' \tag{5}$$

where $I_P(\tau,\mu)$ is the radiance at optical depth $\tau$ ($d\tau=K_edz$, with extinction coefficient $K_e$ and layer depth $dz$) in direction $\mu$ for polarization status $P$ (horizontal or vertical), $\omega_0$ is the single scattering albedo of a soil particle, $B(\tau)$ is the Planck function and $P_{ij}$ ($i$, $j$=H or V) is the scattering phase function. The 4-stream fast model proposed by Liu (1998) solves (5) by using the discrete ordinate method and assuming that no cross-polarization exist. The

Henyey-Greenstein formula (Henyey & Greenstein 1941) is used to express the scattering phase function.

3. Volume scattering effects of dry soil particles

With considering the facts that the soil particles are densely compacted, the multi-scattering effects of soil particles should be accounted for. In our algorithm, this volume scattering effect was calculated by the so-called dense media radiative transfer theory (DMRT) under Quasi Crystalline Approximation with Coherent Potential (QCA-CP) (Wen et al. 1990; Tsang & Kong 2001). Dense Media radiative transfer theory was derived from Dyson's equation under the quasi-crystalline approximation with coherent potential (QCA-CP) and the Bethe-Salpeter equation under the ladder approximation of correlated scatterers.

By using the DMRT, the extinction coefficient $K_e$ and albedo $\omega$ used in equation (5) were calculated. And then the radiance of each soil slab was calculated by the 4-stream fast model. The radiance just below the soil/air interface was obtained by integrating the radiance from bottom layer to the top layer. Finally, the apparent emission of soil media, $T_{bs}$ in equation (1) and (2), was obtained.

### 2.1.3. Surface roughness effects

When an electromagnetic wave reaches the air/soil interface, it suffers the reflection and refraction due to the dielectric constant changing in the two sides of the interface. The roughness of the interface divides the reflected wave into two parts, one is reflected in the specular direction and another is scattered in all directions. Generally, the specular component is often referred to as the coherent scattering component. And the scattered component is known as the diffuse or noncoherent component, which consists of power scattered in all directions but with a smaller magnitude than that of the coherent component. Qualitatively, Surface roughness increases the apparent emissivity of natural surfaces, which is caused by increased scattering due to the increase in surface area of the emitting surfaces. And it was demonstrated by many researches that the surface roughness has a nonnegligible effects on the accuracy of soil moisture retrieval by spaceborne microwave sensors (Oh & Kay 1998; Singh et al. 2003). In general, the surface roughness effects are simulated by two ways: semi-empirical models and fully physical-based models.

1. Semi-empirical models

The semi-empirical models are simply and do not cost too much computation efforts. The parameters used in semi-empirical models are often derived from field observations. Depending on the parameters involved, three different semi-empirical models: Q-H model (Choudhury et al. 1979; Wang & Choudhury 1981), Hp model (Mo & Schmugge 1987; Wegmuller & Matzler 1999; Wigneron et al. 2001) and Qp model (Shi et al. 2005).

2. Fully physical-based model

In our algorithm, we simulated the land surface roughness effect using the Advanced Integral Equation Model (AIEM) (Chen et al. 2003). AIEM is a physically-based model with

only two parameters: standard deviation of the height variations σ (or *rms* height) and surface correlation length *l*. AIEM is an extension of the integral Equation Model (IEM) (Fung, Li & Chen 1992). It has been demonstrated that IEM has a much wider application range for surface roughness conditions than other models such as the Small Perturbation Model (SPM), Physical Optics Model (POM) and Geometric Optics Model (GOM). AIEM improves the calculation accuracy of the scattering coefficient compared with IEM by retaining the absolute phase term in the Green's function.

By coupling AIEM with DMRT (DMRT-AIEM), this radiative transfer model for soil media is fully physically-based. As such, the parameters of DMRT-AIEM, such as the *rms* height, correlation length and soil particle size, have clear physical meanings and their values can be obtained either from field measurement or theoretical calculation.

### 2.1.4. Vegetation masking effects

The existence of canopy layers complicates the electromagnetic radiation which is originally emitted solely by soil layers. The vegetation may absorb or scatter the radiation, but it will also emit its own radiation. The effects of a vegetation layer depend on the vegetation opacity $\tau_c$ and the single scattering albedo of vegetation $\omega_c$ (Schmugge & Jackson 1992). The vegetation opacity in turn is strongly affected by the vegetation columnar water content $W_c$. The relationship can be expressed as (Jackson & Schmugge 1991):

$$\tau_c = \frac{b'\lambda^\chi W_c}{\cos\theta} \tag{6}$$

where $\lambda$ is the wavelength, $\theta$ the incident angle, $W_c$ the vegetation water content. $\chi$ is 1.38 and $b'$ is 9.32.

The single scattering albedo, $\omega_c$, describes the scattering of the emitted radiation by the vegetation. It is a function of plant geometry, and consequently varies according to plant species and associations. The value of it is small in the low frequency microwave region (Paloscia & Pampaloni 1988; Jackson & Oneill 1990). In our algorithm, $\omega_c$ is calculated by

$$\omega_c = \omega_0 \cdot \sqrt{W_c} \tag{7}$$

The value of albedo parameter $\omega_0$ is decided empirically in current researches. Experimental data for this parameter are limited, and values for selected crops have been found to vary from 0.04 to about 0.12.

By combing the $T_{bs}$ solved by equation (5), the surface reflectivity calculated by AIEM, the vegetation opacity $\tau_c$ calculated by equation (6), and the vegetation single scattering albedo $\omega_c$ estimated by equation (7), a physical-based radiative transfer model was developed.

## 2.2. The algorithm

The basis of our algorithm is a database of brightness temperature and/or some indexes calculated from brightness temperature. By searching the data base (or look up table) with

the satellite observation as the input, soil moisture and other related variables of interest can be estimated quickly. Such high searching speed is the main reason why we adopt the look up table method for soil moisture retrieval. The implementation of our algorithm consists of three steps: (1) Fixing the parameters used in the forward model; (2) Generating a look up table by running forward model; and (3) retrieving soil moisture by searching the look up table.

### 2.2.1. Parameterization

As in other physically-based algorithms, such as that developed by Njoku et al. (2003) and the single channel algorithm developed by Jackson (1993), the parameters used in our algorithm have clear physical meanings. This advantage derives from the strength of the forward radiative transfer model. Before running the forward RTM to generate look up table, the parameters should be confirmed at first. The parameters to be confirmed include *rms* height ($h$), correlation length ($l$), soil particle sizes ($r$) and vegetation parameters such as $\chi$ and $b'$. Currently, we can obtain these parameters through the best-fitting method.

For the region where in-situ soil moisture and temperature observation are available and when such observation are also representative, we can use a best-fitting way to optimize parameters. In order to simplify the calculation, low frequencies simulation and observation were used. These parameters are optimized by minimizing the cost function:

$$J(h,l,r,b',\chi,...) = \sum_{i=1}^{n} \sum_{f} \sum_{p=H,V} ABS[TB_{sim}(i,f,p) - TB_{obs}(i,f,p)] \tag{8}$$

where the subscript *sim* denotes the model simulated value and *obs* is the observed value. $n$ is the number of samples used in the optimization. $p$ denotes the polarization status: $H$ for horizontal polarization and $V$ for vertical. $f$ is some frequency in the long wavelength region where the atmospheric effect may be ignored, such as 6.9, 10.7 and 18.7 GHz of AMSR-E, 1.4 GHz of SMOS and 19GHz of SSM/I.

### 2.2.2. Look up table generation

After Step 1, the optimal parameter values are then stored in the forward RTM. We then run the forward model by inputting all possible values of variables used in Equation (1), such as soil moisture content, soil temperature, vegetation water content and atmosphere optical thickness. A family of brightness temperatures is then generated. Based on this brightness temperature database, we select brightness temperatures of special frequencies and polarization to compile a lookup table or to calculate some indices to compile a lookup table. For example, in order to partly remove the influences of physical temperature, the ratio of brightness temperature at different frequencies and polarizations can be used. For instant, we can compile a look up table by using the index of soil wetness (ISW) (Koike et al. 1996; Lu et al. 2009), and Polarization Index (PI) (Paloscia & Pampaloni 1988).

$$PI(19) = \frac{TB(19,V) - TB(19,H)}{TB(19,V) + TB(19,H)} \tag{9}$$

$$ISW(19,37) = \frac{TB(37,H) - TB(19,H)}{TB(37,H) + TB(19,H)} \qquad (10)$$

where TB(19, V) and TB(19, H)and represents the brightness temperature observed at
19GHz vertical and horizontal   polarization channel, respectively, TB(37,H) is the
observation at 37GHz horizontal polarization channel.

### 2.2.3. Soil moisture estimation

The lookup table generated in Step 2 is reversed to give a relationship which maps the
brightness temperature or indices obtained from satellite remote sensing data to the
variables of interest (such as soil moisture, soil temperature and vegetation water content).
Finally, we estimate soil moisture content by linear interpolation of the brightness
temperature or indices into the inverted lookup table.

## 2.3. Ancillary data sets

In order to run forward model, various parameters are needed. These parameters are
provided from ancillary data set. Soil parameters, including soil texture and bulk density are
from FAO data set. Vegetation parameters used in calculated optical thickness are from
references and vegetation types. Land cover map is also used to identify the regions with
dense vegetation and big water surface, where the current soil moisture retrieval algorithm
is not applicable.

# 3. Study regions and used data

## 3.1. Study regions

Africa continent, comparing to the other continent in the world, is less impacted by industry
development. There is the largest desert of the world and the arid-like climate is dominative
in the most part of Africa continent. Therefore, Africa continent has an environment
vulnerable to climate change. On the other hand, it is very difficult to monitor the
environmental changes in this region due to its tough situations and less-development.

In this study, the application region is covered the whole Africa continent, from 20W to 60E
and from 40S to 40N. The application period is from 1988 to 2007, which is the period
covered by SSM/I observation.

## 3.2. Reanalysis data

In this study, due to the limitation of in situ observation data in Africa, only the numerical
model output is available for the results inter-comparison. The current general circulation
models (GCM) are mainly focusing on the atmospheric variable simulation. However, the
surface soil moisture simulations are not as reliable as atmospheric variables (Li, Robock &

Wild 2007).  From a view of water budget, the land surface water comes from atmosphere, controlled by the precipitation and radiation. Consequently, we use the atmospheric variables from the reanalysis data to express the land surface wetness change. The variable used in representing climate change tendency is the net water flux at the land surface, which represents the vertical water budget in the atmosphere as:

$$W_{net} = E - P \tag{11}$$

where $W_{net}$ is the net water flux, $E$ is the evaportranspiration flux and $P$ is the precipitation flux. The positive value of net water flux means drying situation, while the negative value represents wetting trends. In order to partly mitigate the bias inherited in the individual GCM, two sets of reanalysis data, ERA-40 and NCEP, were used in this study.

ERA-40 is a reanalysis of meteorological observations  produced by the European Centre for Medium-Range Weather Forecasts (ECMWF) (Uppala et al. 2005). The ERA-40 has a TL159 horizontal resolution and 60 vertical levels. The ERA-40 dataset used in this study has been obtained from the ECMWF data server (http://data.ecmwf.int/data/d/era40_daily/).

The National Centers for Environmental Prediction/National Center for Atmospheric Research (NCEP/NCAR) reanalysis (which is referred to as the NCEP reanalysis hereafter) is a global reanalysis that was initiated in 1948 and continues to the near real-time at a horizontal resolution of T62 and a temporal resolution of 6 hours (Kalnay et al. 1996). The dynamic model that is used in the NCEP reanalysis is the NCEP global spectral model (Kalnay, Kanamitsu & Baker 1990; Karamitsu 1989; Kanamitsu et al. 1991), in which the land surface processes are treated as portions of the atmospheric model in a relatively simple approach.

### 3.3. SSM/I remote sensing data

The brightness temperature of SSM/I observed at 19.35 GHz and 37GHz was used as the observation data in this research. The SSM/I is flown by the Defense Meteorological Satellite Program (DMSP) on two operational polar orbiting platforms. The first spacecraft of SSM/I series (F08) was launch in June 1987. Currently working one is the F17 launch in December 2006. TABLE I gives the launch date and end date of SSM/I satellites.

The nadir angle for the Earth-viewing reflector of SSM/I is $45°$, which results in an Earth incidence angle of $53.4° \pm 0.25°$. The lower frequency channels (19, 22, and 37 GHz) are sampled so that the pixel spacing is 25 km, and the 85 GHz channels are sampled at 12.5 km pixel spacing. More information on the SSM/I can be found in (Hollinger et al. 1987). The brightness temperature data of SSM/I is archived in the National Snow and Ice Data Center (NSIDC) (Armstrong et al. 2012). The brightness temperature data used in this research can be found at the following webpage: http://nsidc.org/data/docs/daac/nsidc0032_ssmi _ease_tbs.gd.html.

| Satellite | Launch Date | End Date |
|---|---|---|
| F08 | July 1987 | December 1991 |
| F10 | December 1990 | November 1997 |
| F11 | December 1991 | May 2000 |
| F13 | May 1995 | November 2009 |
| F14 | May 1997 | August 2008 |
| F15 | December 1999 | |
| F16 | October 2003 | |
| F17 | December 2006 | |

**Table 1.** SSM/I Launch Dates and End Dates

## 4. Results and discussions

Using the algorithm, daily soil moisture was retrieved from SSM/I TB data. The daily soil moisture is then converted into monthly average soil moisture data set. Figure 1 shows the monthly averaged soil moisture data at July of 1988.
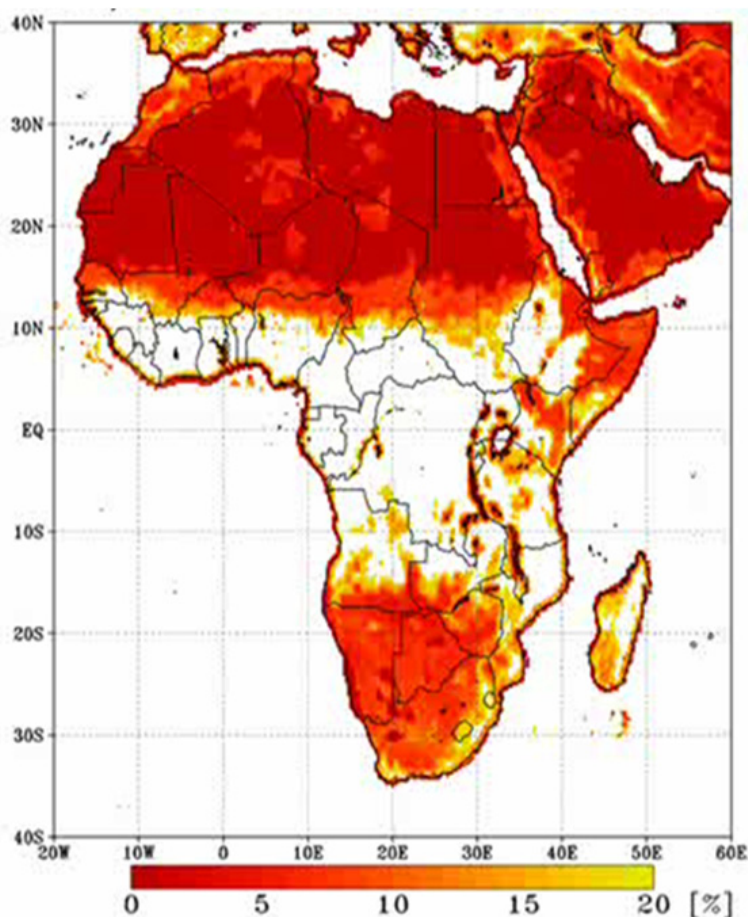


**Figure 1.** Retrieved montly averaged soil  moisture from SSM/I

From Figure 1, it is clear that the retrieved soil moisture over Africa is less than 20%., which may be an underestimation. But the distribution patterns are in a realistic ways: (1) coastal regions generally show larger values than inland regions; (2) the desert regions have the smallest values; (3) the South Africa is wetter than North Africa, because July is the winter month and raining season of South Africa.

In central Africa regions, retrieval algorithm failed to estimate soil moisture values from SSM/I observation. It is because the vegetation is very dense in these regions and the microwave signal could not penetrate the canopy layers and failed to reach the soil layer. For such regions with dense vegetation, longer wavelength channel observation is needed to detect land surface information.

## 4.1. Climate change tendency

In order to identify the climate change tendency, long term averaged data were used. We first divided 20 years soil moisture data into two groups: the first decade from 1988 to 1997 and the second decade from 1998 to 2007.And then we calculated the decade-average summer soil moisture for each decade. It means ten years average of JJA (June, July, and August) for northern hemisphere and of DJF (December, January, and February) for southern hemisphere. Finally, we calculated the difference between the second decade-average and the first decade-average.
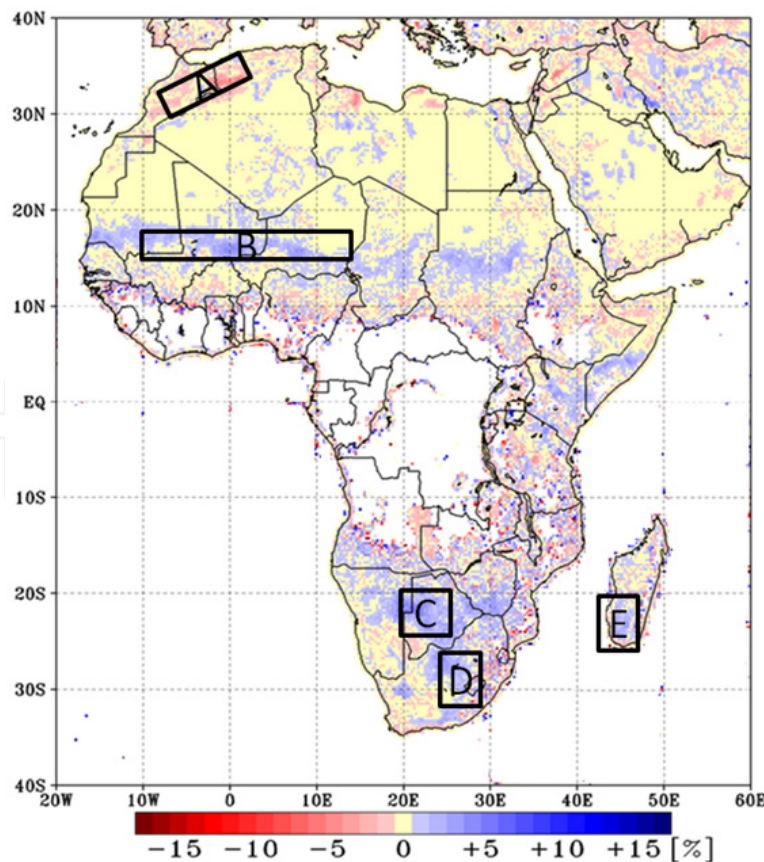


**Figure 2.** Difference between two decade-average summer soil moisture (%)

Figure 2 shows the difference between (1998~2007) and (1988~1997). From this figure, we can identify some climate change tendencies over the Africa continent:

**1.   There is a drying tendency in the coastal regions of Mediterranean Sea:**

These regions include: Morocco, Algeria, Tunisia, and Libya. The drying tendency in region A is most remarkable. This finding is in agreement with the report of Esper et al. (2007): the drought occurrence frequency in Morocco is increasing during last decade.
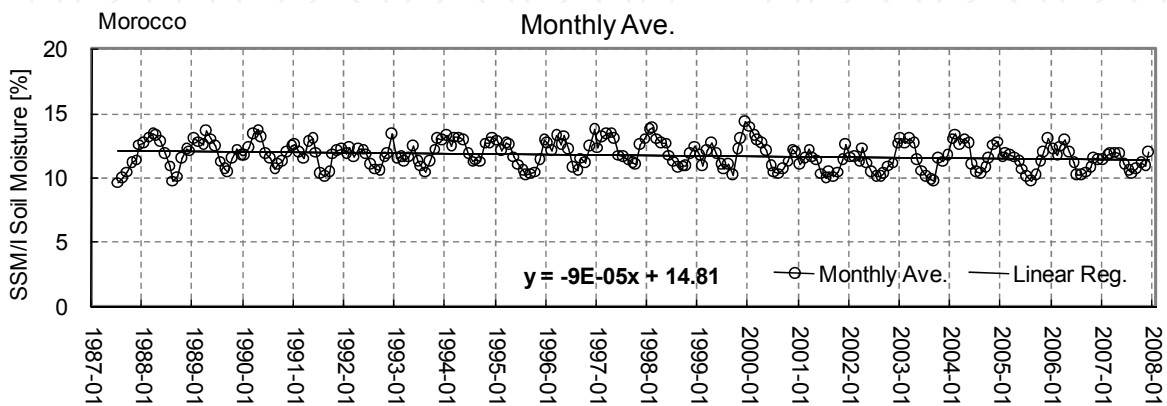


**Figure 3.** Monthly averaged soil moisture at region A from 1987-2008

Figure 3 shows the monthly averaged soil moisture time series for the region A in figure 2. It represents the area-averaged soil moisture variation in Morocco. A linear regression line is also shown in figure 3. The inter-annual variation of soil moisture is not obvious while the maximum values of each year decreases obviously. The regression slope for the region A (-0.00009) is less than zero. It means the surface soil moisture in this region decreases constantly.

**2.   There is a wetting tendency in the belt region from 14N to18N**

It is the south boundary of the Sahara desert, and its land cover type is grassland. Countries located in this region are: Mauritania, Mali, Niger, Chad, Senegal and Sudan. The wetting tendency in region B as marked in the figure is the most remarkable in this belt.
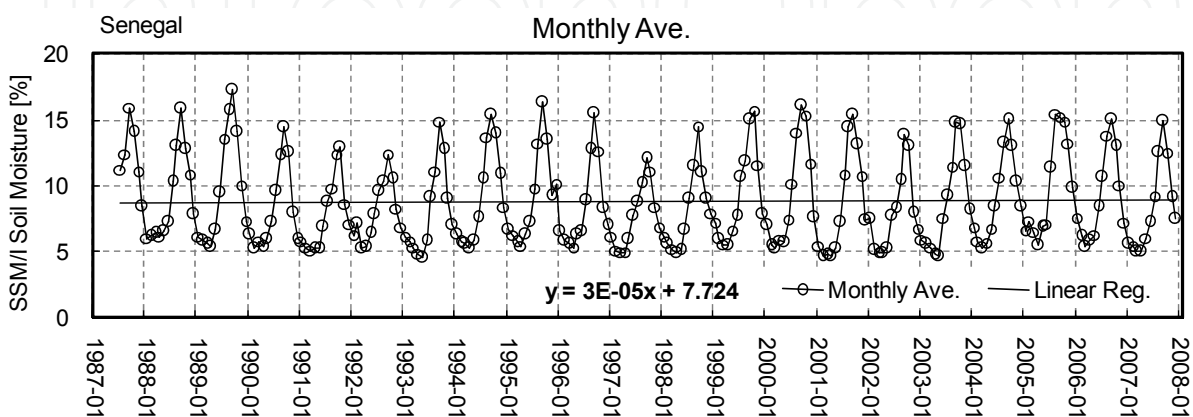


**Figure 4.** Monthly averaged soil moisture at region B from 1987-2008

Figure 4 shows the monthly averaged soil moisture time series in Senegal. It is clear form figure 4 that the second decade is wetter than the first decade, with less inter-annual varation. The linear regression slope in figure 4 (0.00003) is larger than 0, meaning that the surface soil moisture increases constantly during 1987-2008.

## 3. There is a general wetting tendency in the South Africa region

Countries showing such tendency include: Namibia, Botswana, Zimbabwe, and South Africa, marked as regions C and D in figure 2. Region C is located in the Kalahari Desert, which showing most remarkable wetting tendency. The main land cover type of region C is savanna.
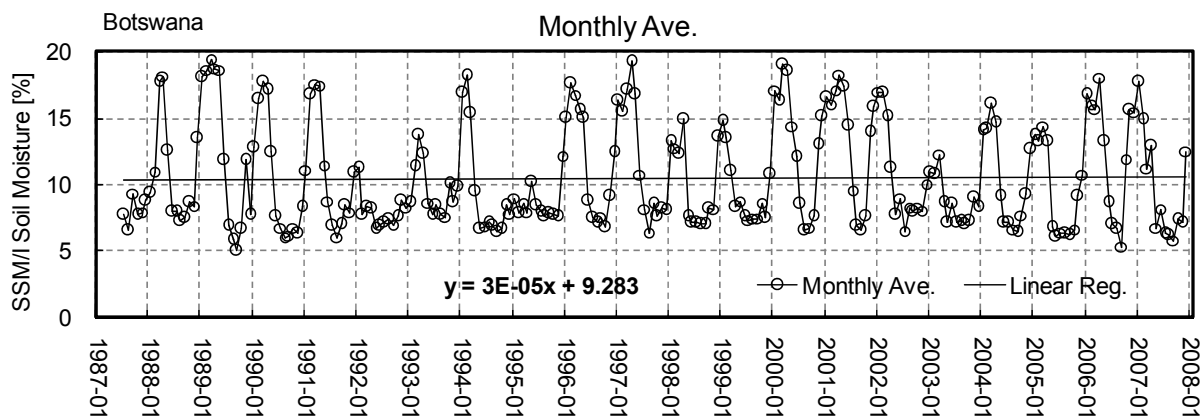


**Figure 5.** Monthly averaged soil moisture at region C from 1987-2008

Figure 5 shows the soil moisture time series in Botswana of region C. During the first decade (1988-1997), there are three years with extreme dry situation, while there only one year during the second decade. The linear regression slope of region C is larger than zero and it means soil moisture increases in this region for the last 20 years. It is mainly a result of less extreme dry years in the second decade.

## 4. There is a slight wetting tendency in the southern part of Madagascar Island
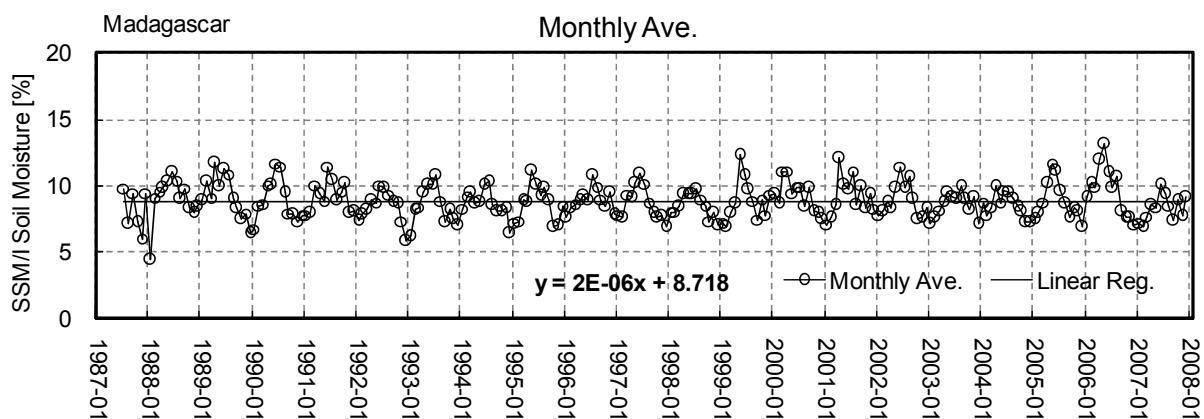


**Figure 6.** Monthly averaged soil moisture at region E from 1987-2008

As shown in figure 6, there are four wet anomaly years in the second decade, i.e. 1999, 2001, 2005 and 2006. The linear regions slope of this region is also larger than zero. It means the soil moisture in region E increases during last 20 years and it mainly due to more anomaly wet years in recent 10 years.

## 4.2. Comparison to ERA-40

Figure 7 presents 20 years averaged summer (*E-P*) over the continent, calculated from ERA-40 reanalysis data. Comparing with Figure 2, the same wetting tendency in region B, C, D and E can be identified easily. The findings from remote sensing data are in good agreement with the reanalysis data.

As shown in Figure 7, the wetting tendency is remarkable in the tropical region. But current remote sensing data failed to provide soil surface information in this region. We cannot identify any remarkable drying tendency in the coast region along Mediterranean Sea.
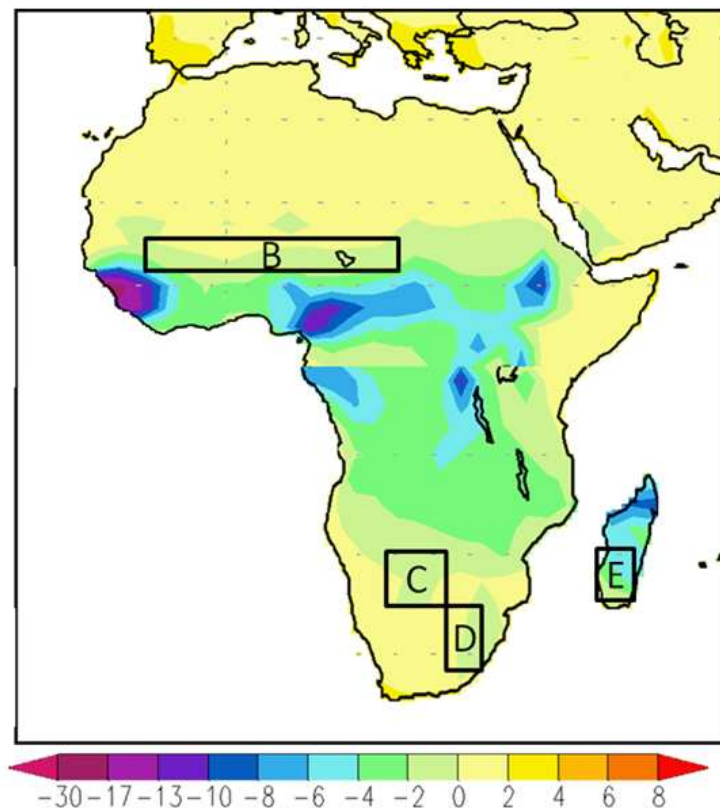


**Figure 7.** 20 years averaged (E-P) from ERA-40 (unit: mm)

It means that the drying trend in Morocco is not significant in ERA-40 data. By using only ERA-40, the land surface wetness change trends in Morocco will be missed. It means that remote sensing data is able to provide complementary climate change information to the traditional reanalysis data. Moreover, the climate change trend derived from ERA-40 shows a wet bias over the whole Africa continent.

### 4.3. Comparison to NCEP

As discussed in the introduction part, all numerical models have limitation. In order to overcome the shortage of individual model, inter-comparison of multi-model results were proposed in this research. Beside ERA-40, NCEP reanalysis data was also used to check the performance of remote sensing results.

Figure 8 shows the 20 years averaged net water flux over Africa by using NCEP reanalysis data. Comparing Figure 8 with Figure 2, both remote sensing data and NCEP data show the drying trends in region A and the wetting trends in region D and E. But NCEP data failed to represent the wetting trends in region B and C. Comparing Figure 8 with 7, both the area and absolute values of the wetting regions of NCEP data is much smaller than those of ERA-40. It suggests that the climate change trend derived from NCEP data shows a dry bias over the continent.
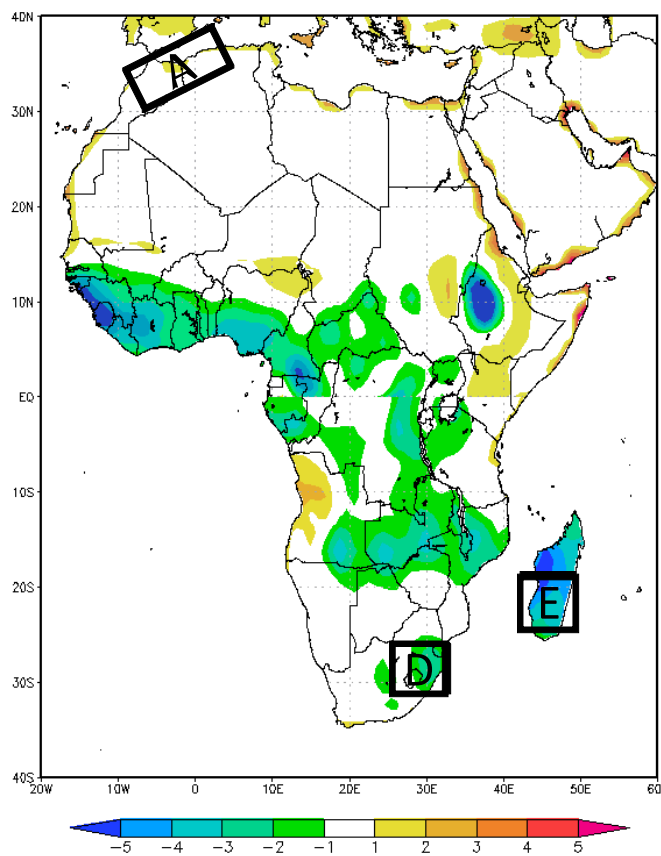


**Figure 8.** Long-term net water flux over Africa from NCEP (unit:mm)

## 5. Conclusions

Spatial distributed soil moisture information is an essential parameter for hydrological, meteorological and ecological studies. In this paper, we developed a 20-year soil moisture data set over Africa continent by using a soil moisture retrieval algorithm which estimated soil moisture from passive microwave remote sensing data provided by SSM/I.

Using this long-term soil moisture data set, some climate change tendencies were indentified:

- There is a remarkable drying trend in the north part of Morocco and Libya, which is verified by local observation. The surface soil moisture in this region decreases constantly with small inter-annual variations during last 20 years. This drying trend is also captured by the NCEP reanalysis data.

- There is a wetting belt in the south boundary of Sahara desert, including Mauritania, Mali, Niger, Chad, Senegal and Sudan. The surface soil moisture in this region increases constantly with small inter-annual variation during past 10 years. This wetting trend is also captured by the ERA-40 reanalysis data.

- There is a general wetting tendency in South Africa region, including the Kalahari Desert. From the viewpoint of land cover, grass land and savanna region is getting wet. Such wetting tendencies are in good agreement with the analysis results of ERA-40 reanalysis data. NCEP reanalysis data also shows a wetting trend in parts of this domain (region D). The wetting trend in this region is mainly a result of less extreme dry years in the second decade.

- There is a wetting trend in the south of Madagascar Island, which is also captured by both ERA-40 and NCEP data. The wetting trends in the island it mainly due to more anomaly wet years in recent 10 years.

This study demonstrates that passive microwave remote sensing data is able to provide independent and complementary land surface information to the climate change research. It is a kind of "observation" data, which does not rely on any model assumption and initial conditions. As shown in the results from ERA-40 and NCEP, model simulations have some biases and fail to capture all climate change information over the whole continent. Remote sensing data, therefore, could provide independent and complementary information in climate change study.

But there are some limitations in current remote sensing data, for example, it cannot provide soil information in dense vegetation region. This shortage can be partly overcome as the launch of Soil Moisture and Ocean Salinity mission (SMOS) (Kerr et al. 2001) and future coming Soil Moisture Active and Passive mission (SMAP) (Entekhabi et al. 2008). L band microwave observation which has a longer wavelength will be available and the shadowing effects of vegetation could be gradually alleviated. In addition to the adoption of new sensors, merging remote sensing data and land surface models into a Land Data Assimilation System (LDAS) (Reichle & Koster 2005) is highly expected to the maximum usage of remote sensing data and our knowledge of climate systems.

The data used in this study covers the period from 1987 to 2008. The soil moisture spatiotemporal variation characteristics derived from this research are therefore just from a short period of 20 years. By integrating the remote sensing observations made by SMMR, SSM/I, Tropical Rainfall Measuring Mission Microwave Imager (Jackson & Hsu 2001), AMSR-E and oncoming Global Change Observation Mission – Water (Imaoka et al. 2010) with the proposed ensemble method, a long term soil moisture time series

beginning in 1978 can be reconstructed. Such a long-term remote sensing data set has high potential in the assessment of global change impacts on water resources, agriculture, and ecology.

## Author details

Hui Lu
*Ministry of Education Key Laboratory for Earth System Modeling, and Center for Earth System Science, Tsinghua University, Beijing, China*

Toshio Koike, Tetsu Ohta and Katsunori Tamagawa
*The Department of Civil Engineering, The University of Tokyo, Tokyo, Japan*

Hideyuki Fujii
*Earth Observation Research Center, Japan Aerospace Exploration Agency, Ibaraki, Japan*

David Kuria
*Geomatic Engineering and Geospatial Information Science Department, Kimathi University College of Technology, Kenya*

## Acknowledgement

## 6. References

Armstrong RL, Knowles KW, Brodzik MJ, Hardman MA 2012, DMSP SSM/I-SSMIS Pathfinder Daily EASE-Grid Brightness Temperatures. Boulder, Colorado USA: National Snow and Ice Data Center. Digital media.

Betts AK, Ball JH, Beljaars ACM & Viterbo PA 1996, 'The land surface-atmosphere interaction: a review based on observational and global modeling perspectives', *Journal of Geophysical Research*, vol. 101, pp. 7209–7225.

Beljaars ACM, Viterbo P, Miller MJ & Betts AJ 1996, 'The anomalous rainfall over the United States during July 1993: sensitivity to land surface parameterization and soil moisture anomalies', *Monthly Weather Review*, vol. 124, pp. 362-383.

Burke, WJ, Schmugge TJ & Paris JF 1979, 'Comparison of 2.8 and 21 cm microwave radiometer observations over soils with emission model calculation', *Journal of Geophysics Research*, vol. 84, pp. 287-294.

Chen KS, Wu TD, Tsang L, Li Q, Shi JC & Fung AK 2003, 'Emission of rough surfaces calculated by the integral equation method with comparison to three-dimensional moment method simulations', *IEEE Transactions on Geoscience and Remote Sensing*, vol. 41, pp. 90-101.

Choudhury BJ, Schmugge TJ, Chang ATC & Newton NR 1979, 'Effect of surface roughness on the microwave emission from soils', *Journal of Geophysical Research,* vol. 84, pp. 5699-5706.

Delworth T & Manabe S 1988, 'The influence of potential evaporation on the variability of simulated soil wetness and climate', *Journal of Climate*, vol. 13, pp. 2900–2922.

Dobson MC, Ulaby FT, Hallikainen MT & Elrayes MA 1985, 'Microwave dielectric behavior of wet soil 2: dielectric mixing models', *IEEE Transactions on Geoscience and Remote Sensing*, vol. 23, pp. 35-46.

Entekhabi D, Njoku E, O'Neill P, Spencer M, Jackson T, Entin J & Kellogg EIm K 2008, 'The Soil Moisture Active/Passive Mission (SMAP)', *IEEE Geoscience and Remote Sensing Symposium 2008 (IGARSS08)*, vol. 3, pp. 1-4.

Entekhabi D, Rodrigues-Iturbe I & Castelli F 1996, 'Mutual interaction of soil moisture state and atmospheric processes', *Journal of Hydrology*, vol. 184, pp. 3-17.

Esper J, Frank D, Bu¨ntgen U, Verstege A, Luterbacher J & Xoplaki E 2007, 'Long-term drought severity variations in Morocco', *Geophysical Research Letters,* vol. 34, pp.1-5.

Fung AK, Li ZQ & Chen KS 1992, 'Backscattering from a randomly rough dielectric surface.', *IEEE Transactions on Geoscience and Remote Sensing*, vol. 30, pp. 356-369.

Gillies RR & Carlson TN 1995, 'Thermal remote sensing of surface soil water content with partial vegetation cover for incorporation into climate models', *Journal of Applied Meteorology*, vol. 34, pp. 745-756.

Gloersen, P & Barath FT 1977, 'A Scanning Multichannel Microwave Radiometer for Nimbus-G and SeaSat-A', *IEEE Journal of Oceanic Engineering*, vol. 2, pp.172-178.

Henyey LC & Greenstein JL 1941, 'Diffuse radiation in the galaxy', *The Astrophysics Journal*, vol. 93, pp. 70–83.

Hipp J.E. 1974, 'Soil electromagnetic parameters as functions of frequency, soil density, and soil moisture', *Proceedings of the IEEE*, vol. 62, pp.98–103

Hollinger J, Lo R, Poe G, Savage R & Pierce J 1987, 'Special Sensor Microwave/Imager user's guide', NRL Tech. Rpt., Naval Research Laboratory, Washington, DC, 120 p.

Imaoka K, Kachi M, Fujii H, Marakami H, Hori M, Ono A, Igarashi T, Nakagawa K, Oki T, Hoda Y & Shimoda H 2010, 'Global change observation mission (GCOM) for monitoring carbon, water cycles and climate change', *Proceedings of IEEE*, vol. 98, pp. 717-734.

Jackson TJ 1993, 'Measuring surface soil moisture using passive microwave remote sensing', *Hydrology Processes,* vol. 7, pp. 139-152.

Jackson TJ 1997, 'Soil moisture estimation using special satellite microwave/imager satellite data over a grassland region', *Water Resources Research*, vol. 33, pp.1475-1484.

Jackson TJ & Hsu AY. 2001, 'Soil moisture and TRMM microwave imager relationships in the Southern Great Plains 1999 (SGP99) experiment', *IEEE Transactions on Geoscience and Remote Sensing*, vol. 39, pp. 1632-1642

Jackson TJ & Oneill PE 1990, 'Attenuation of Soil Microwave Emission by Corn and Soybeans at 1.4 Ghz and 5 Ghz', *IEEE Transactions on Geoscience and Remote Sensing*, vol. 28, pp. 978-980.

Jackson TJ & Schmugge TJ 1991, 'Vegetation effects on the microwave emission of soils', *Remote Sensing of Environment*, vol. 36, pp. 203-212.

Kalnay E, Kanamitsu M & Baker WE 1990, 'Global numerical weather prediction at the National Meteorological Center', *Bulletin of the American Meteorological Society*, vol. 71, pp. 1410-1428.

Kalnay E, Kanamitsu M, Kistler R, Collins W, Deaven,D, Gandin L, Iredell M, Saha S, White G, Woollen J, Zhu Y, Chelliah M, Ebisuzaki W, Higgins W, Janowiak J, Mo KC, Ropelewski C, Wang J, Leetmaa A, Reynolds R, Jenne R & Joseph D 1996, 'The NCEP/NCAR 40-year reanalysis project', *Bulletin of the American Meteorological Society*, vol. 77, pp. 437-471.

Kanamitsu M 1989, 'Description of the NMC global data assimilation and forecast system', *Weather and Forecasting*,  vol. 4, pp. 335-342.

Kanamitsu M, Alpert JC, Campana KA, Caplan PM, Deaven DG, Iredell M, Katz B, Pan HL, Sela J & White GH 1991, 'Recent changes implemented into the global forecast system at NMC',  *Weather and Forecasting*, vol. 6, pp. 425-435.

Kerr YH, Waldteufel P, Wigneron JP, et al. 2001, 'Soil moisture retrieval from space: the soil moisture and ocean salinity (SMOS) mission. I*EEE Transactions on Geoscience and Remote Sensing*, vol. 39, pp. 1729-1735.

Koike T, Tsukamoto T, Kumakura T & Lu M 1996, 'Spatial and seasonal distribution of surface wetness derived from satellite data', *Proceedings of International workshop on macro-scale hydrological modeling*, pp. 87-96.

Li H, Robock A & Wild M 2007, 'Evaluation of Intergovernmental Panel on Climate Change Fourth Assessment soil moisture simulations for the second half of the twentieth century', *Journal of Geophysical Research*, vol. 112, D06106, doi:10.1029/2006JD007455

Liu, G 1998, 'A fast and accurate model for microwave radiance calculations', *Journal of Meteorology  Society of Japan*, vol. 76, pp. 335–343.

Lu H, Koike T, Fujii H, Ohta T & Tamagawa K 2009, 'Development of a Physically-based Soil Moisture Retrieval Algorithm for Spaceborne Passive Microwave Radiometers and its Application to AMSR-E', *Journal of The Remote Sensing Society of Japan*, vol. 29, pp. 253-261.

Melillo JM, Steudler PA, Aber JD, Newkirk K, Lux H, Bowles FP, Catricala C, Magill A, Ahrens T & Morrisseau S 2002, 'Soil warming and carbon-cycle feedbacks to the climate system, *Science*,  vol. 298, pp. 2173-2176.

Mo T & Schmugge TJ 1987, 'A Parameterization of the Effect of Surface-Roughness on Microwave Emission', *IEEE Transactions on Geoscience and Remote Sensing*, vol. 25, pp. 481-486

Njoku EG & Chan SK 2006, 'Vegetation and surface roughness effects on AMSR-E land observations', *Remote Sensing of Environment*, vol. 100, pp. 190-199.

Njoku EG & Entekhabi D.1996, 'Passive microwave remote sensing of soil moisture', *Journal of Hydrology*, vol.184, pp.101-129.

Njoku EG, Jackson TJ, Lakshmi V, Chan TK & Nghiem SV 2003, 'Soil moisture retrieval from AMSR-E', *IEEE Transactions on Geoscience and Remote Sensing, vol.* 41, pp. 215-229.

Njoku, EG &  Li L 1999, 'Retrieval of land surface parameters using passive microwave measurements at 6-18 GHz', *IEEE Transactions on Geoscience and Remote Sensing*, vol. 37, pp. 79-93.

Oh Y & Kay YC 1998, 'Condition for precise measurement of soil surface roughness', *IEEE Transactions on Geoscience and Remote Sensing*, vol. 36, pp. 691-695.

Oh Y, Sarabandi K & Ulaby FT 1992, 'An emperical-model and an inversion technique for Radar scattering from bare soil surfaces', *IEEE Transactions on Geoscience and Remote Sensing*, vol. 30, pp.370-381.

Paloscia S, Macelloni G & Santi E 2006, 'Soil moisture estimates from AMSR-E brightness temperatures by using a dual-frequency algorithm', *IEEE Transactions on Geoscience and Remote Sensing*, vol. 44, pp. 3135-3144.

Paloscia S, Macelloni G., Santi E & Koike T. 2001, 'A multifrequency algorithm for the retrieval of soil moisture on a large scale using microwave data from SMMR and SSM/I satellites', *IEEE Transactions on Geoscience and Remote Sensing*, vol. 39, pp.1655-1661.

Paloscia S & Pampaloni P 1988, 'Microwave polarization index for monitoring vegetation growth', *IEEE Transactions on Geoscience and Remote Sensing*, vol. 26, pp. 617-621.

Paloscia, S., Pampaloni, P., Pettinato, S. & Santi, E. 2008, 'A comparison of algorithms for retrieving soil moisture from ENVISAT/ASAR images', *IEEE Transactions on Geoscience and Remote Sensing*, vol. 46, pp. 3274-3284.

Pastor J & Post WM 1986, 'Influence of climate, soil-moisture, and  succession on forest carbon and nitrogen cycles', *Biogeochemistry*, vol. 2, pp. 3-27.

Prigent C, Aires F, Rossow WB & Robock A 2005, 'Sensitivity of satellite microwave and infrared observations to soil moisture at a global scale: Relationship of satellite observations to in situ soil moisture measurements', *Journal of Geophysical Research*, vol. 110, D07110. doi:10.1029/2004JD005087

Prigent C, Wigneron JP, Rossow WB & Pardo-Carrion JR 2000, 'Frequency and angular variations of land surface microwave emissivities: Can we estimate SSM/T and AMSU emissivities from SSM/I emissivities?', *IEEE Transactions on Geoscience and Remote Sensing*, vol. 38, pp.2373-2386.

Ray, PS 1972, 'Broadband Complex Refractive Indices of Ice and Water', *Applied Optics* vol. 11,  pp.1836-1844.

Reichle RH & Koster RD 2005, 'Global assimilation of satellite surface soil moisture retrievals into the NASA catchment land surface model', *Geophysics research letters*, vol. 32,  doi:10.1029/2004GL021700.

Schar C, Luthi D, Beyerle U & Heise E 1999, 'The soil-precipitation feedback: A process study with a regional climate model', *Journal of Climate*, vol. 12, pp.722–741.

Schmugge TJ & Jackson TJ 1992, 'A Dielectric Model of the Vegetation Effects on the Microwave Emission from Soils', *IEEE Transactions on Geoscience and Remote Sensing*, vol. 30, pp. 757-760.

Schmugge, TJ & Choudhury BJ 1981, 'A comparison of radiative transfer models for predicting the microwave emission from soils', *Radio Science*, vol. 16, pp. 927-938.

Seneviratne, SI, Luthi D, Litschi M & Schar C 2006, 'Land–atmosphere coupling and climate change in Europe', *Nature*, vol. 443, pp. 205–209.

Shi JC, Jiang LM, Zhang LX, Chen KS, Wigneron JP & Chanzy A 2005, 'A parameterized multifrequency-polarization surface emission model', *IEEE Transactions on Geoscience and Remote Sensing*, vol. 43, pp. 2831-2841.

Singh D, Sing KP, Herlin I & Sharma SK 2003, 'Ground-based scatterometer measurements of periodic surface roughness and correlation length for remote sensing', *Advances in Space Research*, vol. 32, pp. 2281-2286.

Tsang L & Kong JA 1977, 'Theory for thermal microwave emission from a bounded medium containing spherical scatterers', *Journal of Applied Physics*, vol. 48, pp. 3593-3599.

Tsang L & Kong JA 2001, *Scattering of Electomagnetic Waves: Advanced Topics*, Wiley, New York.

Uppala SM, Kållberg PW, Simmons AJ, Andrae U, V. da Costa Bechtold & Fiorino M 2005, 'The ERA-40 re-analysis', *Quarterly Journal of the Royal Meteorological Society*. Vol. 131, pp.2961–3012.

Verstraeten WW, Veroustraete F, van der Sande CJ, Grootaers I & Feyen J 2006, 'Soil moisture retrieval using thermal inertia, determined with visible and thermal spaceborne data, validated for European forests', *Remote Sensing of Environment*, vol. 101, pp. 299-314.

Wagner W, Scipal K, Pathe C, Gerten D, Lucht W & Rudolf B 2003, 'Evaluation of the agreement between the first global remotely sensed soil moisture data with model and precipitation data', *Journal of Geophysical Research*, vol. 108, pp. 4611- , doi:10.1029/2003JD003663

Wang JR & Choudhury BJ 1981, 'Remote-Sensing of Soil-Moisture Content over Bare Field at 1.4 Ghz Frequency', *Journal of Geophysical Research-Oceans and Atmospheres*, vol. 86, pp. 5277-5282.

Wang, J.R. & Schmugge, T.J. 1980, 'An empirical model for the complex dielectric permittivity of soils as a function of water content', *IEEE Transactions on Geoscience and Remote Sensing*, vol. 18, pp. 288-295.

Wegmuller U & Matzler, C 1999, 'Rough bare soil reflectivity model', *IEEE Transactions on Geoscience and Remote Sensing*, vol. 37, pp. 1391-1395.

Wen B, Tsang L, Winebrenner DP & shimura A 1990, 'Dense media radiative transfer theory: comparison with experiment and application to microwave remote sensing and polarimetry', *IEEE Transactions on Geoscience and Remote Sensing*, vol. 28, pp. 46-59.

Wigneron J. P., Schmugge T., Chanzy A., Calvet J. C. & Kerr Y. 1998, 'Use of passive microwave remote sensing to monitor soil moisture', *Agronomie*, vol.18, pp. 27-43.

Wigneron J.P., Laguerre L & Kerr Y 2001, 'A simple parameterization of the L-band microwave emission from rough agricultural soils', *IEEE Transactions on Geoscience and Remote Sensing*, vol. 39, pp. 1697-1707.